



# FAILURE ANALYSIS OF A UAV FLIGHT CONTROL SYSTEM USING MARKOV ANALYSIS

E. G. Okafor<sup>1,\*</sup> and I. H. Eze<sup>2</sup>

<sup>1,2</sup>AIR FORCE INSTITUTE OF TECHNOLOGY, NAF BASE, KADUNA, KADUNA STATE, NIGERIA

*Email addresses:* <sup>1</sup>[eg.okafor@gmail.com](mailto:eg.okafor@gmail.com), <sup>2</sup> [hillaryeze40@yahoo.com](mailto:hillaryeze40@yahoo.com)

## ABSTRACT

*Failure analysis of a flight control system proposed for Air Force Institute of Technology (AFIT) Unmanned Aerial Vehicle (UAV) was studied using Markov Analysis (MA). It was perceived that understanding of the number of failure states and the probability of being in those state are of paramount importance in order to ensure safety flight of the UAV. Thus, in this study the number of working states and the probability of being in those states for the proposed UAV flight control system was accessed using Markov Analysis (MA). Specifically, the truncated transition state diagram of the UAV flight control system considered in this study was developed and differential equations associated with the transition state diagram were also generated. Laplace transformation technique was used to solve the differential equations. From the findings of the study, the need for design improvement was established.*

**Keywords:** *Failure analysis, Markov analysis, Flight control system, Reliability block diagram, and State transition diagram*

## 1. INTRODUCTION

Safety analysis is an important obligation to demonstrate compliance with airworthiness requirement for airborne systems. At present, Fault Tree Analysis (FTA), Dependence Diagram Analysis (DDA) and Markov Analysis (MA) are the most widely-used methods of probabilistic safety and reliability analysis for airborne system [1].

Fault trees analysis is a backward failure searching technique which starts form a top event and can provide quantitative results such as the top event probability or qualitative results in the form of Minimum Cut Sets (MCS) via combination of identified causes and Boolean gates. In FTA and DDA it is difficult to permit for various types of failure modes and dependencies such as transient and intermittent faults, coincident- faults and standby systems with spares. Also an FTA is constructed to assess cause and probability of a single top event. When a system has many failure conditions, separate fault trees may need to be constructed for each one of them making the process cumbersome [2].

In some cases, it may also be very difficult for a fault tree to represent the system completely. Examples of systems that are difficult to model using FTA or DD

include repairable systems and systems where failure/repair rates are state dependent. However, Markov Analysis technique can be used to accurately model system with varied failure scenario such as those described above [1]. Sequence dependent events are included naturally; therefore MA can cover a wide range of system behaviors [3]. Thus, in this study MA was used.

MA has been used to model dynamics of large-scale grid systems [4]. In the study, A Markov chain model of a grid system was first represented in a reduced, compact form, which was then perturbed to produce alternative system execution paths and identify scenarios in which system performance is likely to degrade or anomalous behaviors occur. The authors further stressed that the expeditious generation of these scenarios allows prediction of how a larger system will react to failures or high stress conditions [4]. Farsad et al implemented a Markov channel model to reduce the simulation time necessary for studying Active Transport Molecular Communication (ATMC) without sacrificing accuracy [5].

It is globally a continuous effort to design Unmanned Aerial Vehicles (UAVs) for special military or civil missions [6-7]. The main missions of interest for UAVs

\*Corresponding author, Tel: +234-816-660-5114

are surveillance, detection, communication and deployment of war-heads. The advantages of a UAV include quick deployment, real-time data, low radar cross-section, transportable by a single operator and low production cost in comparison to conventional military or civil aircraft. Development of UAVs places key emphasis on data communication, on-board navigation, propulsion, flight control systems and airframe aerodynamics. This paper focuses on UAV flight control system.

Chen et al studied the Probabilistic Safety Analysis of a Flight Control System based on Bayesian Network [8]. Their results revealed that the Bayesian Network provide a simple and intuitive measure to deal with the safety analysis of flight control system with multi-state property.

For the UAV to carry out these missions, its flight control system has to be inherently reliable. Little is known on the application of Markov Analysis techniques for the failure analysis of UAV's flight control systems. Hence, in order to ascertain the reliability of a proposed UAV flight control system design to be adopted for the Air Force Institute of Technology (AFIT), Nigerian Air Force (NAF) base, Kaduna ABT-18 UAV project, this paper, implements Markov analysis as a tool for the failure analysis of the ABT-18 UAV flight control system.

**2. PROPOSED AFIT UAV FLIGHT CONTROL SYSTEM**

The flight control system shown in Figure 1 and analysed in this research work was a modified conventional aircraft flight control system proposed for the AFIT UAV project [9].

As may be seen from Figure 1, the control commands from the ground control station drive the control surfaces (rudder, elevator, and flap) through the control actuators which augment the available power to overcome the aerodynamic loads on the control surfaces.

There are two feedback loops which draw their control signals from motion sensors that meets the requirements of the control laws. The outputs from the inner and outer loop controllers are summed up electronically and the resultant signal will control the aircraft through a servo actuator. The servo actuator is an electro mechanical device which converts low power electrical signals to mechanical signals at a power level compatible with the control commands from the ground station.

Also, the inner loop of the flight control system is the stability augmentation system (SAS), which is an electro mechanical device that senses the undesirable motion of the aircraft and then moves the appropriate controls to damp out the motion. It is an automatic control system that has the capability of stabilizing or improving the stability of the UAV against any undesirable attitude or motion of the UAV. Therefore, SAS is inherently built into the airframe to augment the effect of undesirable motion.

The outer loop is the autopilot; on activation, the autopilot automatically controls all the flight manoeuvres. It is usually incorporated for precision flight manoeuvres where the aircraft is required to fly under adverse conditions and also to temporally relief the ground control operator at the ground station of their duties.

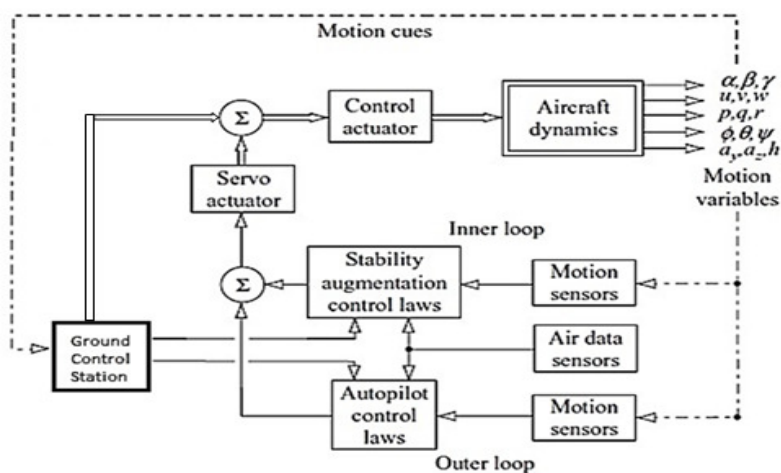


Figure 1 AFIT proposed UAV flight control system [9]

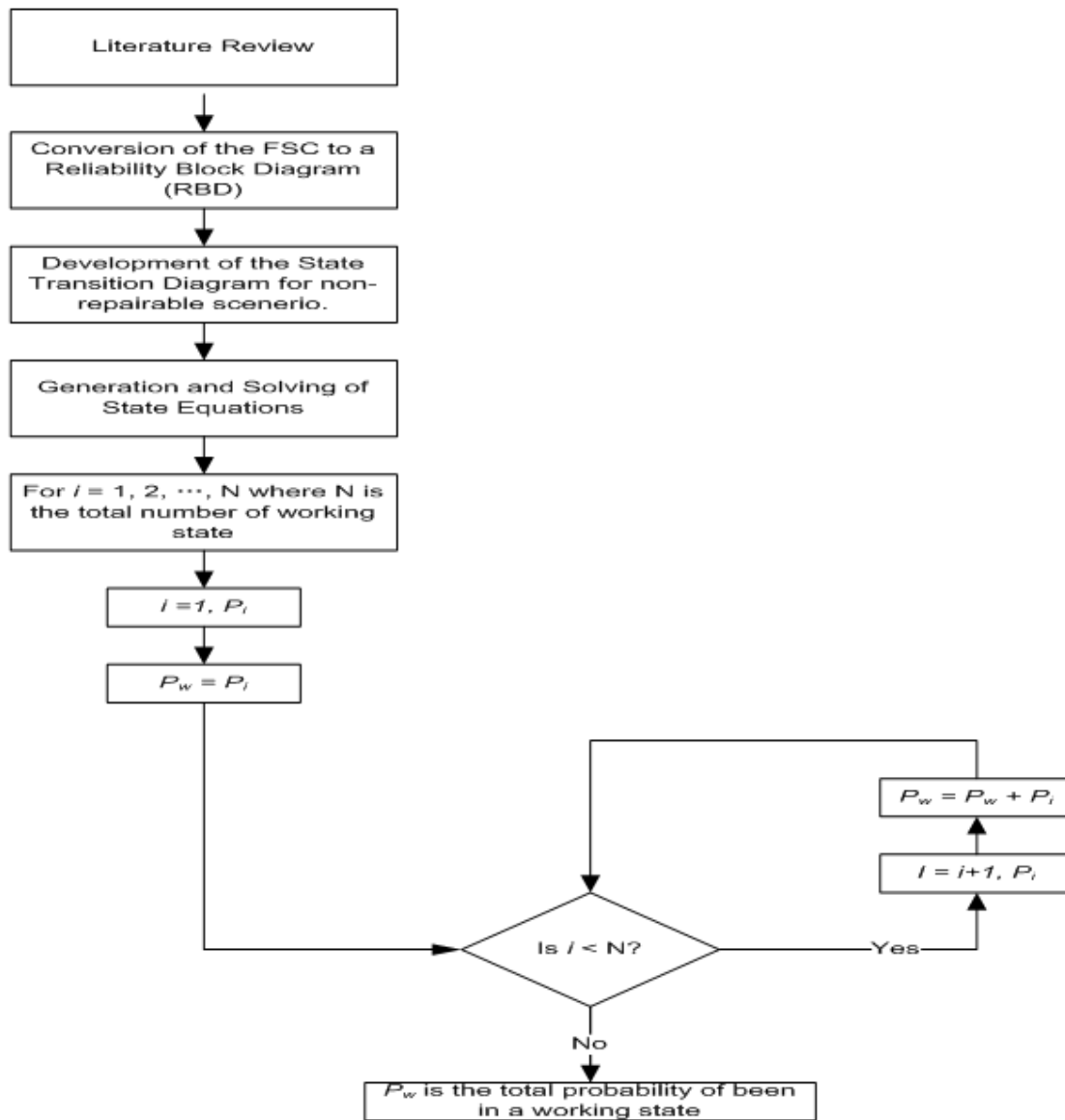


Figure 2 Research flowchart

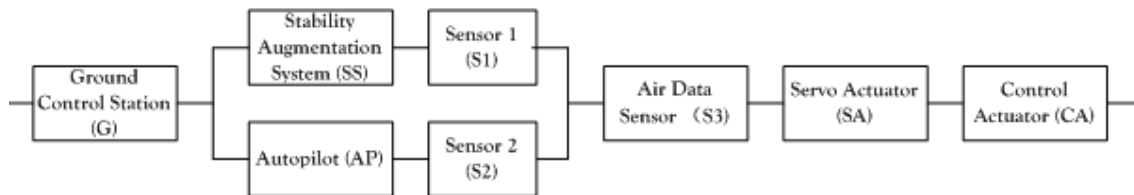


Figure 3 FCS Reliability Block Diagram

**3. METHODOLOGY**

**3.1 Research Method**

The step by step approach used to achieve the objectives of this research work is depicted in the flow chart shown in Figure 2. From Figure 2, literature review was conducted in area beneficial to the focus of this work. Following an extensive literature review, the UAV flight control system proposed for AFIT UAV

project [9] was converted to reliability block diagram (RBD).

The RBD was then used to develop the Markov transition state diagram for non-repairable scenario. Using the Markov state transition diagram, state equations were developed and solved implementing Laplace transformation. The sum of the probability of all working states associated with the FCS represents

the reliability or the probability of working at the time considered in this study.

**3.2 Conversion of the Flight Control System to Reliability Block Diagram (RBD)**

The construction of the state reliability block diagram (RBD) for the above flight control system shown in Figure 3 was based on adequate analysis of the functional connections that exist between FCS components.

The components considered are the two motion (S1 and S2) and air data (S3) sensors, the stability augmentation system (SS), the servo actuator (SA), autopilot (AP), ground control system (G) and the control actuator (CA). The two motion sensors are responsible for the feed loops. It gets feedback from the motion variables (the actual deflection state or position of the control surfaces) and sends the signals to stability augmentation system for appropriate action.



The stability augmentation system (SS) and autopilot (AP) receives feedback signal from the motion sensors, one for each. Thus, the SS and AP are connected in series with one motion sensor. This type of connection indicates that the failure of the stability augmentation system and autopilot will result to operational failure of the entire FCS.

The servo actuator main function is to sum up the output signals from the outer and inner loops respectively, and transmits same to control actuator so as to enable the actual deflection of the control surfaces. Therefore, the SS, SA, CA, G and S3 are all in series connection to each other because; any of these components failure simply implies the failure of the FCS.

**3.3 State Transition Diagram**

Using the RBD shown in Figure 3, the state transition diagram was developed for non-repairable scenario. The non-repairable scenario considered in this work simply implies that failure of the component or system was not repaired. A description of the symbols used in this study is shown in table 3.1

*Table 1 Description of Markov analysis symbols*

S/N	Symbols	Name	Meaning
1		State	Represents system state
2		Connecting Edge	Connects one state to another
3	$\lambda$	Failure Rate	Failure rate of a component

The transition state diagram in this work was developed by implementing the steps described below:

- Step 1** Begin at the left of the diagram with state (circle) identified as  $S_1$ . All components or equipment are operationally good at this state.
- Step 2** Study the consequence of failing each element in each of its failure modes. Group as a common consequence any that result in removing the same element from operation
- Step 3** Assign new state and identify  $S_2, S_3, S_4, \dots, S_n$  for unique consequence of step 2.
- Step 4** Connect arrow from  $S_1$  to each of the new states and note on each arrow the failure rate or rates of the element or elements whose failure determined transition to the new state.
- Step 5** Repeat step 2, 3, and 4 for each of the new state failing only the elements still operational in that state.
- Step 6** Continue the process until the initial system is totally non-operational.

Truncated MA transition diagram was implemented, based on the premise that a failed system does not necessarily mean all system components has failed. Thus each of the transition diagram path was terminated or truncated at the state in which a system failure can be established.

**3.4 State Equation**

The Markov differential state equations were developed by describing the probability of being in each system state  $S_1, S_2, S_3, \dots, S_n$  at time  $t + \Delta t$  as a function of the state of the system at time  $t$ . The number of state in the transition state diagram is equal to the number of state equations. The state equation in this work was developed adopting conditions stated below.

**Condition 1**

*The probability of being in state  $S_n$  where  $n = 1$  at time  $t + \Delta t$ . This is equal to the probability of being in state  $S_n$  at time  $t$  and not transitioning out during  $\Delta t$ .*

**Condition 2**

*The probability of being in any state  $S_n$  where  $n > 1$  at time  $t + \Delta t$ . This is equal to the sum of the probability of being in all preceding states at time  $t$  and transitioning to  $S_n$  at time  $\Delta t$  plus the probability of being in state  $S_n$  at time  $t$  and transitioning out during  $\Delta t$ .*

Solving the state equation for a given state gives the probability of being in that state. In this work, Laplace transformation was used to solve the states differential equations obtained. The sum of the

probability of all working state gives the FCS reliability or the probability of being in a working state.

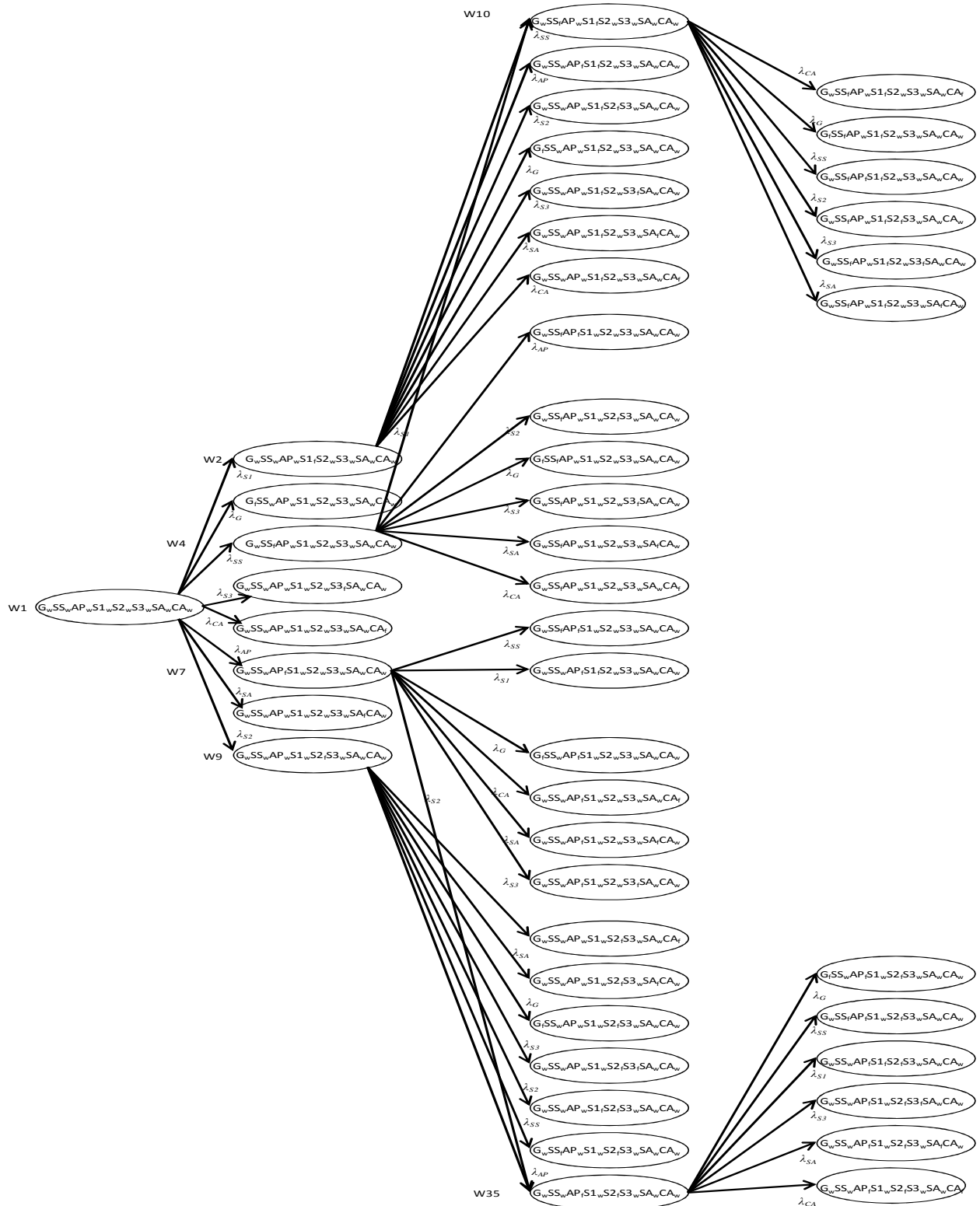


Figure 4 Truncated FCS transition state diagram

**3.5 Parameter Setting**

Using failure rate data contained in Non- Electronic Parts Reliability Data (NPRD 1991), the failure rate of the position sensors (S1 and S2), air data sensor (S3) control actuators (CA) and servo actuator (SA) of  $90.46 \times 10^{-6}$ ,  $0.3328 \times 10^{-6}$ ,  $4.144 \times 10^{-6}$ , and  $1.29 \times 10^{-6}$  respectively were used. The stability augmentation system (SS), autopilot (AP), and ground control system (G) failure rate of  $1.521 \times 10^{-8}$ ,  $1 \times 10^{-8}$ , and  $1 \times 10^{-9}$  were assumed based on the fact that such systems are usually very reliable. Assuming 40 working hours a week and 50 working weeks a year and warranty period of five years, the total operational time for the FCS in five years was found to be 10,000hours. This time used for the probability computation in this work of 10,000hours was reached.

**4. RESULT**

**4.1 State Transition Diagram**

Based on the methods described in section 3.4, the transition state diagram obtained is shown in Figure 4.

From Figure 4, 47 states was reached. These forty seven states represent a truncated state transition diagram. Usually, for eight components series or mixed system configuration,  $2^8$  (256) states are required. The value of the probability of being in a working state will not change irrespective of whether the truncated or a complete configuration diagram is used. Therefore, truncated state transition diagram was used in this work. Seve of the 47 states represented in Figure 4 represents the possible working state. These states are state 1, 2, 4, 7, 9, 10 and 35. The sum of the probability of being in state 1, 2, 4, 7, 9, 10 and 35 becomes the probability of the FCS being in a working state.

**4.2 State Equations and Analysis**

Using the conditions stated in section 3.4, the state equation for each working state (W1, W2, W4, W7, W9, W10, W35) shown in Figure 4 was obtained as depicted in equation (1)-(7).

$$\begin{aligned}
 P_1(t + \Delta t) &= P_1(t) \cdot [1 - (\lambda_G + \lambda_{AP} + \lambda_{SS} + \lambda_{S1} + \lambda_{S2} + \lambda_{S3} + \lambda_{SA} + \lambda_{CA})] \Delta t & (1) \\
 P_2(t + \Delta t) &= P_1(t) \cdot \lambda_{S1} \Delta t + P_2(t) [1 - (\lambda_G + \lambda_{AP} + \lambda_{SS} + \lambda_{S2} + \lambda_{S3} + \lambda_{SA} + \lambda_{CA})] \Delta t & (2) \\
 P_4(t + \Delta t) &= P_1(t) \cdot \lambda_{SS} \Delta t + P_2(t) [1 - (\lambda_G + \lambda_{S1} + \lambda_{AP} + \lambda_{S2} + \lambda_{S3} + \lambda_{SA} + \lambda_{CA})] \Delta t & (3) \\
 P_7(t + \Delta t) &= P_1(t) \cdot \lambda_{AP} \Delta t + P_2(t) [1 - (\lambda_G + \lambda_{S1} + \lambda_{SS} + \lambda_{S2} + \lambda_{S3} + \lambda_{SA} + \lambda_{CA})] \Delta t & (4) \\
 P_9(t + \Delta t) &= P_1(t) \cdot \lambda_{S2} \Delta t + P_2(t) [1 - (\lambda_G + \lambda_{S1} + \lambda_{SS} + \lambda_{AP} + \lambda_{S3} + \lambda_{SA} + \lambda_{CA})] \Delta t & (5) \\
 P_{10}(t + \Delta t) &= P_2(t) \cdot \lambda_{SS} \Delta t + P_4(t) \cdot \lambda_{S1} \Delta t + P_{10}(t) [1 - (\lambda_G + \lambda_{AP} + \lambda_{S2} + \lambda_{S3} + \lambda_{SA} + \lambda_{CA})] \Delta t & (6) \\
 P_{35}(t + \Delta t) &= P_7(t) \cdot \lambda_{S2} \Delta t + P_9(t) \cdot \lambda_{AP} \Delta t + P_{35}(t) [1 - (\lambda_G + \lambda_{SS} + \lambda_{S1} + \lambda_{S3} + \lambda_{SA} + \lambda_{CA})] \Delta t & (7)
 \end{aligned}$$

Implementing Laplace transformation on equation 1-7 and set the probability of being in state one (1) at time zero (0) as  $P_1(0) = 1$ , while the probability of being in state  $n$  where  $n > 1$  at time zero (0) as  $P_n(0) = 0$ , then the probability of being in state 1, 2, 4, 7, 9, 10 and 35 was reached as represented in equation (8)-(14).

$$\begin{aligned}
 P_1(t) &= e^{-(\lambda_G + \lambda_{SS} + \lambda_{AP} + \lambda_{S1} + \lambda_{S2} + \lambda_{S3} + \lambda_{SA} + \lambda_{CA})t} & (8) \\
 P_2(t) &= e^{-(\lambda_G + \lambda_{SS} + \lambda_{AP} + \lambda_{S2} + \lambda_{S3} + \lambda_{SA} + \lambda_{CA})t} - e^{-(\lambda_G + \lambda_{SS} + \lambda_{AP} + \lambda_{S1} + \lambda_{S2} + \lambda_{S3} + \lambda_{SA} + \lambda_{CA})t} & (9) \\
 P_4(t) &= e^{-(\lambda_G + \lambda_{AP} + \lambda_{S1} + \lambda_{S2} + \lambda_{S3} + \lambda_{SA} + \lambda_{CA})t} - e^{-(\lambda_G + \lambda_{SS} + \lambda_{AP} + \lambda_{S1} + \lambda_{S2} + \lambda_{S3} + \lambda_{SA} + \lambda_{CA})t} & (10) \\
 P_7(t) &= e^{-(\lambda_G + \lambda_{SS} + \lambda_{S1} + \lambda_{S2} + \lambda_{S3} + \lambda_{SA} + \lambda_{CA})t} - e^{-(\lambda_G + \lambda_{SS} + \lambda_{AP} + \lambda_{S1} + \lambda_{S2} + \lambda_{S3} + \lambda_{SA} + \lambda_{CA})t} & (11) \\
 P_9(t) &= e^{-(\lambda_G + \lambda_{SS} + \lambda_{AP} + \lambda_{S1} + \lambda_{S3} + \lambda_{SA} + \lambda_{CA})t} - e^{-(\lambda_G + \lambda_{SS} + \lambda_{AP} + \lambda_{S1} + \lambda_{S2} + \lambda_{S3} + \lambda_{SA} + \lambda_{CA})t} & (12) \\
 P_{10}(t) &= \frac{\lambda_{S1}}{\lambda_{S1} + \lambda_{SS}} e^{-(\lambda_G + \lambda_{S3} + \lambda_{AP} + \lambda_{S2} + \lambda_{SA} + \lambda_{CA})t} + \frac{\lambda_{SS}}{\lambda_{S1} + \lambda_{SS}} e^{-(\lambda_G + \lambda_{SS} + \lambda_{AP} + \lambda_{S1} + \lambda_{S2} + \lambda_{S3} + \lambda_{SA} + \lambda_{CA})t} \\
 &+ \frac{\lambda_{SS}}{\lambda_{S1} + \lambda_{SS}} e^{-(\lambda_G + \lambda_{S3} + \lambda_{AP} + \lambda_{S2} + \lambda_{SA} + \lambda_{CA})t} + \frac{\lambda_{S1}}{\lambda_{S1} + \lambda_{SS}} e^{-(\lambda_G + \lambda_{SS} + \lambda_{AP} + \lambda_{S1} + \lambda_{S2} + \lambda_{S3} + \lambda_{SA} + \lambda_{CA})t} \\
 &- e^{-(\lambda_G + \lambda_{SS} + \lambda_{AP} + \lambda_{S2} + \lambda_{S3} + \lambda_{SA} + \lambda_{CA})t} - e^{-(\lambda_G + \lambda_{AP} + \lambda_{S1} + \lambda_{S2} + \lambda_{S3} + \lambda_{SA} + \lambda_{CA})t} & (13) \\
 P_{35}(t) &= \frac{\lambda_{S2}}{\lambda_{S2} + \lambda_{AP}} e^{-(\lambda_G + \lambda_{S3} + \lambda_{SS} + \lambda_{S1} + \lambda_{SA} + \lambda_{CA})t} + \frac{\lambda_{AP}}{\lambda_{S2} + \lambda_{AP}} e^{-(\lambda_G + \lambda_{SS} + \lambda_{AP} + \lambda_{S1} + \lambda_{S2} + \lambda_{S3} + \lambda_{SA} + \lambda_{CA})t} \\
 &+ \frac{\lambda_{AP}}{\lambda_{S2} + \lambda_{AP}} e^{-(\lambda_G + \lambda_{S3} + \lambda_{SS} + \lambda_{S1} + \lambda_{SA} + \lambda_{CA})t} + \frac{\lambda_{S2}}{\lambda_{S2} + \lambda_{AP}} e^{-(\lambda_G + \lambda_{SS} + \lambda_{AP} + \lambda_{S1} + \lambda_{S2} + \lambda_{S3} + \lambda_{SA} + \lambda_{CA})t} \\
 &- e^{-(\lambda_G + \lambda_{SS} + \lambda_{S1} + \lambda_{S2} + \lambda_{S3} + \lambda_{SA} + \lambda_{CA})t} - e^{-(\lambda_G + \lambda_{AP} + \lambda_{S1} + \lambda_{SS} + \lambda_{S3} + \lambda_{SA} + \lambda_{CA})t} & (14)
 \end{aligned}$$

Inserting the failure rates of components and time as indicated in section 3.5, the probability of being in states 1, 2, 4, 7, 9, 10 and 35 was found to be 0.1625, 0.239, 0.00002, 0.0001, 0.239, 0 and 0 respectively. Summation of these states probability values, gave the probability of the FCS being in a working state of 0.64. Based on the result obtained it is evident that the reliability of the proposed FCS is low, thus design improvement of components (extremely low failure rates) or adoption of a more robust system configuration may be beneficial in improving the reliability or the probability of being in a working state.

### 5. CONCLUSION AND RECOMMENDATION

In this work, failure analysis of an AFIT proposed UAV Flight Control System was studied. Markov Analysis was used to conduct the failure analysis. From the truncated flight control system transition state diagram developed a total 47 states were observed corresponding to 7 and 40 working and failed states respectively. Also, the probability of being in a working state was found to be 0.64.

Based on the findings of this study, there is a need for design improvement to increase the reliability of the system. Also application of Markov analysis technique used in this study to other UAV sub-systems failure analysis would be very beneficial for accurate failure modelling.

### REFERENCES

- [1] SAE ARP4761 Guideline and Methods for Conducting the Safety Assessment Process on Civil Airborne Systems and Equipment, SAE, 1996.12.
- [2] Vesely W. E., Goldberg F. F., Roberts N. H., HaasID. F. Fault Tree Handbook. *U.S. Nuclear Regulatory Commission*, 1981.
- [3] Louise M. R. Dependency Modeling Using Fault-tree and Cause-Consequence Analysis, *Doctoral Thesis, Loughborough University*, UK, 2000.
- [4] Christopher Dabrowski and Fern Hunt Markov Chain Analysis for Large-Scale Grid Systems *National Institute of Standards and Technology, U.S. Department of Commerce, NISTIR 7566*, April 2009.
- [5] Farsad, N., Eckford, A.W., Hiyama, S. A. Markov Chain Channel Model for Active Transport Molecular Communication. *IEEE Transaction on Signal Processing*, 62 (9); 2014.
- [6] Joseph J. K., Ryan C., Rick L., Andrew J. K. Maneuvering and Tracking for a Micro Air Vehicle using Vision-Based Feedback. *SAE International Paper No. 2004-01-3137*, 2004.
- [7] Joel M.G, Matthew T. K. Development of the Black Widow Micro Air Vehicle, *AIAA-2001-0127*, 2001.
- [8] Chen K., Lu Z., Zeng H. Research on Probabilistic Safety Analysis Approach of Flight Control System based on Bayesian Network, *Procedia Engineering* 00 (2014) 000-000
- [9] Eze I.H., Failure Analysis of a UAV Flight Control System using Markov Analysis, *PGD Thesis, Air Force Institute of Technology (AFIT), Nigeria* 2015.